

# Intracluster light at $z \sim 0.25$ from SDSS imaging data

Stefano Zibetti<sup>1</sup> and Simon D. M. White<sup>1</sup>

<sup>1</sup>Max-Planck-Institut für Astrophysik, Garching bei München, Germany  
email: zibetti@mpa-garching.mpg.de

**Abstract.** We investigate the broadband optical emission of diffuse intergalactic stars in galaxy clusters at  $z \sim 0.25$  by means of an image stacking technique. The images of 654 clusters, selected with the max-BCG algorithm from a subsample of the SDSS-Data Release 1 (DR1), have been stacked after masking all the sources detected down to very low S/N. The resulting images in the g, r and i bands provide reliable photometric data at the level of  $\gtrsim 30 \text{ mag}/\square''$  (r band), out to  $\gtrsim 600$  kpc from the Brightest Cluster Galaxy (BCG).

Our analysis shows that:

- i) the IntraCluster Light (ICL) is much more concentrated than the galaxy light, contributing  $\sim 30\%$  of the total cluster optical emission at  $R = 100$  kpc, but less than 10% at  $R > 500$  kpc;
- ii) the ICL contributes between 15 and 20% of the total cluster optical luminosity between the optical radius ( $\mu_r = 25 \text{ mag}/\square''$ ) of the BCG and 500 kpc;
- iii) the colours of the ICL are consistent with the global colours of the cluster galaxies, with little evidence for redder g-r.

---

## 1. Introduction

Firstly proposed by Zwicky(1951), the presence of a diffuse population of intergalactic stars in galaxy clusters is now a well established observational fact (see e.g. Arnaboldi 2003 and references therein, Krick & Bernstein this conference). Such a population is commonly believed to originate from the disruption of small galaxies and from the tidal stripping of the outskirts of large galaxies in high-density environments. Studying the properties of the ICL as a function of redshift and of the richness and morphology of the parent cluster can give a significant insight in the interaction processes that drive galaxy evolution in dense environments.

Observing the intracluster light (ICL) is extremely challenging, due to the very low surface brightness involved ( $> 26 \text{ mag}/\square''$ ), which is less than 1% of the typical surface brightness of the sky. During the last years the increasing sensitivity of CCD detectors and the development of new observational techniques has made it possible to start a number of optical surveys aiming at the study of the ICL, by means of both broadband imaging of unresolved stellar populations (e.g. Feldmeier *et al.* 2002) and of narrow band detection of intracluster planetary nebulae (e.g. Arnaboldi *et al.* 2003). Nevertheless, for a statistically representative number of clusters of different morphology and richness and located at different redshifts we still lack reliable determinations of the basic properties of the ICL, such as the fractional amount with respect to the total optical emission of the cluster, the radial distribution, the link with (possible) cD envelopes, or the colours. In fact, observations of the ICL in individual clusters are extremely demanding in telescope time and require an incredibly high control of the flat fielding and of the sources of light pollution, such as fore- and background sources and the internal reflections of the camera. We have chosen to tackle the problem with a purely statistical approach, adopting an image stacking technique, similar to that used by Zibetti, White, & Brinkmann (2004).

The Sloan Digital Sky Survey (SDSS, York *et al.* 2000) is providing a one-quarter-of-sky coverage with 5-band imaging (Fukugita *et al.* 1996, Gunn *et al.* 1998) and spectroscopy. From a subsample of its first data release (DR1, Abazajian *et al.* 2003), we have extracted a catalogue of 654 clusters and rich groups in the redshift range 0.2-0.3, whose imaging in the g, r, and i bands was processed and stacked, as described in Sec.2. The results are presented and discussed in Sec.3.

## 2. Method: the stacking technique

The very essence of the stacking technique consists in averaging a large number of images of clusters, in order i) to increase the signal-to-noise ratio and measure surface brightnesses as faint as  $\mu_r \sim 30 \text{ mag}/\square$ , and ii) to statistically remove the effects of flat fielding inhomogeneities and the contamination from scattered light, internal reflections, and fore- and background sources. Given the typical S/N in the SDSS imaging and the limitation imposed by the present day coverage of the survey, a suitable number of images ranges from several hundreds to roughly 1,000.

### 2.1. The SDSS sample

The sample selection focused on clusters in the redshift range 0.2-0.3 for two main reasons. First, we want the spatial extension of the individual clusters not to exceed the dimensions of the frame, since an annulus of at least 1 Mpc around the cluster must be included on the same frame for a reliable background subtraction. Given the size of the SDSS frames, the chosen redshift range represents the best trade-off between this spatial constraint and the desire for minimum cosmological dimming of the apparent surface brightness and for maximum efficiency in detecting galaxies. On the other hand, at  $z = 0.25$  the g-r colour conveniently maps the 4000Å-break, thus providing important information about the intracluster stellar population.

The cluster sample is drawn from  $\sim 1500 \text{ deg}^2$  of photometric data in the SDSS DR1, using the maxBCG method by Annis *et al.* (2004) (see also Bahcall *et al.* 2003 for a description of this technique). We require estimated photometric redshift  $0.2 < z < 0.3$ , 17 or more galaxies identified as red-sequence members within 1 Mpc projected distance† from the BCG, and at least 13 of them within 330 kpc. The clusters selected in this way have richness roughly in the same range as the Abell clusters. Clusters in vicinity of bright foreground stars or in frames contaminated by scattered light have been pruned from the sample.

### 2.2. Image processing

The SDSS imaging data are available as bias subtracted, flat-field corrected frames. For each cluster we estimate the sky background in an annulus of 1 Mpc, 100 kpc thick, centered on the BCG, after masking all the sources detected at very low S/N with SExtractor, in at least one of the three passbands. After subtracting the background, for each image two kinds of masks are built, “ICL” and “galaxy”. The former are obtained from SExtractor segmentation images, adopting fixed surface brightness detection thresholds ( $\mu_r=24.5$ ,  $\mu_g=25.0$ ,  $\mu_i=24.0$ ) and minimum detection area of 10 contiguous pixels. Corrections for galactic extinction and cosmological dimming  $((1+z)^4)$  with respect to the median redshift of the sample are applied. The masks of bright sources are grown by 30 pixels in order to avoid scattered light, while the BCG is left unmasked. The final “ICL”

†  $H_0=70 \text{ km sec}^{-1} \text{ Mpc}^{-1}$ ,  $\Omega_0=1$ ,  $\Omega_\Lambda=0.7$  throughout this paper.

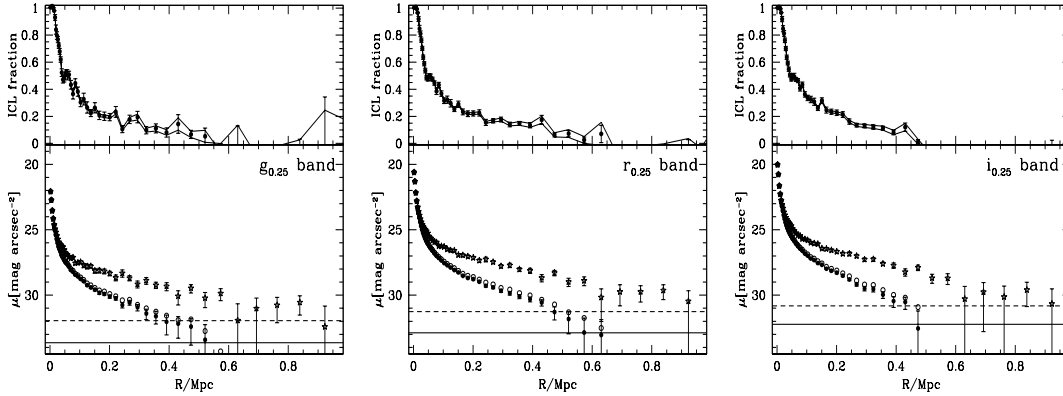


**Figure 1.** Lower panels: SB profiles for the total light (stars), the measured diffuse light (open circles) and the corrected ICL (filled circles). Lines display the background uncertainty for the total light (dashed line) and for the diffuse component (solid line). Errorbars are 1- $\sigma$  errors, including random noise and systematic background uncertainty. Upper panels: the local ICL/total ratio. Errorbars account for random errors only, while the solid lines represent the 1- $\sigma$  intervals when accounting for systematic errors in the background estimation.

mask results from the OR combination of the masks obtained for the three passbands. In the “galaxy” masks only the bright sources are masked.

The images and the corresponding masks are geometrically transformed, centered on the BCG, rescaled to the same physical units and randomly rotated. Finally, the images are averaged excluding the pixels masked according either to the “ICL” or to the “galaxy” masks, so that it is possible to estimate the average contribution from the diffuse light (plus the BCG) and the average total light, respectively.

### 3. Results

In Fig.1 (lower panels) we show the azimuthally averaged SB profiles extracted from the stacked images, after subtracting the background evaluated at 1 Mpc, in g, r, and i band respectively. The star points represent the total cluster light (“galaxy” masks), while the open circles are the diffuse light (“ICL” masks). The solid and the dashed lines display the level of the background uncertainty for the diffuse component and for the total light, respectively. As apparent from these plots, we are able to measure SB $\dagger$  as faint as  $\mu_r \simeq 32$  for the diffuse component, and  $\mu_r \simeq 30$  for the total light, the latter being limited by the shot noise of the background galaxy distribution.

Whether the diffuse light we measure is “true” ICL is questionable, depending on the actual definition of ICL. In principle one should consider as ICL only the light coming from stars which are unbound from individual galaxies and freely fluctuating in the cluster potential. Since this is clearly not a viable operational definition, we consider as ICL all the light coming from outside of the optical radius of galaxies (i.e. the isophotal radius at  $\mu_r = 25$ ). This is a well defined quantity, that can be also easily tested against theoretical predictions. However, due to the magnitude limits of the SDSS ( $m_r = 22.2$ ), we expect significant contribution to the diffuse light from undetected cluster galaxies. We quantify this contamination by simulating a set of mock galaxy clusters, in the same observational conditions (redshift, galactic extinction, seeing) as the observed ones.

$\dagger$  All surface brightnesses are expressed in the observer’s frame filter system for clusters at  $z=0.25$ .

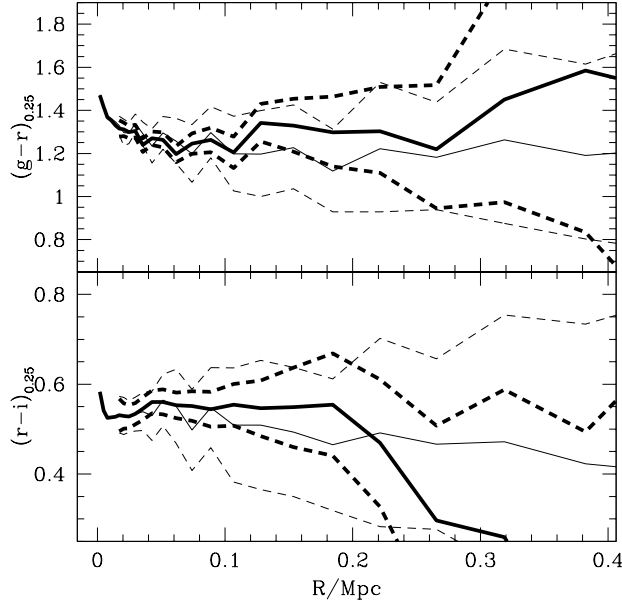


**Figure 2.** g-r and r-i colour profiles. Dashed lines represent the  $1-\sigma$  confidence intervals, thick lines are for the ICL, thin for the total cluster light.

Each simulated cluster includes 1,000 galaxies, whose apparent magnitude is assigned according to a monte-carlo realization of a Schechter luminosity function (LF). We use the distribution of Sersic profile parameters as a function of luminosity as observed by Blanton *et al.* (2003) to create a realistic 2D image of each galaxy, truncated at the  $\mu_r = 25$  isophote. The images are then convolved with the observed PSF, background and poissonian noise are added. After processing and stacking the mock images in the same way as the observed ones, we measure the fraction of galaxy light that is missed by the masking algorithm and contributes to the diffuse component. This fraction depends on the assumed LF, and ranges from a few percent for a flat LF, up to 15% in the case of a steep faint end. Assuming the LF given by Goto *et al.* (2002) ( $M_r^* = -22.21$ ,  $\alpha = -0.85$ ), this fraction is 5% (r band).

The corrected SB of the ICL is represented by filled circles in the lower panels of Fig.1. We find that the ICL is much more concentrated than the total light in the cluster, irrespective of the passband. The local fractional contribution of the ICL is shown in the upper panels of Fig.1. Note that, since we do not mask the BCG, the fraction is 1 in the center. At 100 kpc the fraction of light contributed by the ICL is  $\sim 30\%$ , and drops to  $\sim 5\%$  at 500 kpc. The overall fraction of ICL between the average optical radius of the BCG (30 kpc) and 500 kpc is 20% in the r band, and 19% in the g and i bands, with typical uncertainties of  $\pm 2\%$ . Assuming a steeper LF can lower these figures by up to  $\sim 5\%$ .

Using the three observed bands, we study the g-r and r-i colour profiles of the ICL out to 400 kpc from the BCG. They are shown in Fig. 2 as the thick solid lines. The total-light colours are shown as thin solid lines. Dashed lines display the  $1-\sigma$  confidence intervals. We note a strong negative colour gradient in the central 20 kpc, that is inside the BCG. The outer profiles do not display any significant gradient in the galaxy component, although marginally bluer r-i is measured at larger radii. Neglecting the r-i at  $R > 0.2$

Mpc, whose value is largely undetermined due to the very low signal, we find that the ICL colours are very similar to those of the galaxy component, with perhaps weak evidence for marginally redder g-r.

This result and the strong, non-linear dependence of the ICL surface brightness on the galaxy density, are consistent with the idea of ICL being emitted by passively evolving stellar populations, stripped from the cluster galaxies in the highest density regions.

The forthcoming analysis of a larger sample of clusters (Zibetti *et al.* 2004 in preparation), differentiated according to their richness and morphology (e.g. Bautz-Morgan type), will contribute new clues about the origins of the ICL.

### Acknowledgements

We thank Jim Annis for kindly providing us with the maxBCG catalog of clusters used in this work.

Funding for the creation and distribution of the SDSS Archive has been provided by the Alfred P. Sloan Foundation, the Participating Institutions, the National Aeronautics and Space Administration, the National Science Foundation, the U.S. Department of Energy, the Japanese Monbukagakusho, and the Max Planck Society. The SDSS Web site is <http://www.sdss.org/>. The SDSS is managed by the Astrophysical Research Consortium (ARC) for the Participating Institutions.

### References

- Abazajian, K. *et al.* 2003, *AJ*, **126**, 2081–2086  
Annis, J. *et al.* 2004, in preparation  
Arnaboldi, M. 2003, In *Recycling intergalactic and interstellar matter* (Eds. P. A. Duc, J. Braine, & E. Brinks). IAU Symposium Series, vol. 217 (*astro-ph/0310143*)  
Arnaboldi, M. *et al.* 2003, *AJ*, **125**, 514–524  
Bahcall, N. A. *et al.* 2003, *ApJS*, **148**, 243–274  
Blanton, M. R. *et al.* 2003, *ApJ*, **594**, 186–207  
Goto, T. *et al.* 2002, *PASJ*, **54**, 515–525  
Feldmeier, J. J., Mihos, J. C., Morrison, H. L., Rodney, S. A., & Harding, P. 2002, *ApJ*, **575**, 779–800  
Fukugita, M., Ichikawa, T., Gunn, J. E., Doi, M., Shimasaku, K., & Schneider, D. P. 1996, *AJ*, **111**, 1748–+  
Gunn, J. E., *et al.* 1998, *AJ*, **116**, 3040–3081  
York, D. G. *et al.* 2000, *AJ*, **120**, 1579–1587  
Zibetti, S., White, S. D. M., & Brinkmann, J. 2004, *MNRAS*, **347**, 556–568  
Zibetti, S. *et al.* 2004, in preparation  
Zwicky, F. 1951, *PASP*, **63**, 61–+